arXiv:1212.2008v1 [astro-ph.HE] 10 Dec 2012

Bayesian Approach for a Neutrino Point Source Analysis

Debanjan Bose, Lionel Brayeur, Martin Casier, Geraldina Golup and Nick van Eijndhoven

Vrije Universiteit Brussel, Dienst ELEM
Pleinlaan 2, B-1050 Brussels, Belgium

Abstract

In this paper we present a model independent analysis method following Bayesian statistics to search for neutrinos from point sources. The Bayesian approach allows us to obtain the full probability distribution function for both the background and the signal rate. As such, we have direct access to the signal significance and upper limits. Furthemore, it allows also to account for previous results via the concept of prior information without the need of the *ad hoc* application of trial factors.

In this paper we derive an exact analytical expression for the probability density function for the source rate, and consequently also for the flux, of any steady point source assuming a uniform prior distribution. To investigate the validity of our Bayesian approach, we have applied this method to the public IceCube 40-string configuration data for 10 nearby blazars and have obtained a flux upper limit, which compares very well with the previously published result of IceCube, using the same data set.

Key words: Neutrino Astronomy, Neutrino Telescopes, Active Galactic Nuclei, Gamma Ray Bursts, Bayesian Statistics.

---

1 Introduction

Bayesian approaches [1] are gaining more and more popularity in scientific analyses [2,3,4,5]. In this paper we outline a formalism following Bayesian inference to analyse signals from point sources, such as Active Galactic Nuclei (AGN) and Gamma Ray Bursts (GRBs), using data from neutrino telescopes.

A frequentist approach is based on the long run relative frequency of occurrences in identical repeats of an experiment. Consequently, this can only provide the probability for a certain outcome under the assumption of a specific hypothesis. On the other hand, the Bayesian approach allows us to directly compute the probability of any particular hypothesis or parameter value based on observations. One of the great strengths of Bayesian inference is the ability to incorporate relevant prior information in the analysis. This provides a mechanism for a statistical learning process that automatically takes previous results into account.

2 Bayesian Formalism

We denote by $p(A, B|C)$ the probability for hypothesis A and B to be true under the condition that C is true. The product rule [1], $p(A, B|C) = p(A|C)p(B|A, C) = p(B|C)p(A|B, C)$, directly yields Bayes' theorem [6] :

$$p(A|B, C) = \frac{p(A|C)p(B|A, C)}{p(B|C)}. \tag{1}$$

Bayes' theorem is extremely powerful in hypothesis testing. Consider a hypothesis H, some observed data D and prior information I. Bayes' theorem can then be rewritten as :

$$p(H|D, I) = \frac{p(H|I)p(D|H, I)}{p(D|I)}, \tag{2}$$

where

$p(H|D,I) \equiv$ Posterior probability of hypothesis H.

$p(H|I) \equiv$ Prior probability of hypothesis H.

$p(D|H,I) \equiv$ Likelihood function, $\mathcal{L}(H)$.

$p(D|I) \equiv$ Normalization factor.

From Eq. (2) it is seen that the Bayesian formalism automatically provides a learning process. The first step is to encode our prior state of knowledge into a prior probability $p(H|I)$. Based on the arrival of new data this is then converted into a posterior probability $p(H|D,I)$.

We will apply this approach to the analysis of astrophysical point sources. This method will enable us to obtain the full Probability Density Function (PDF) for the source rate from which we can derive the corresponding flux or an upper limit.

3 Bayesian Assessment of Significance

As outlined above, Bayesian logic allows us to make statements about the probability of various hypotheses in the light of obtained data. Following the developments described in [7], we quantify the degree to which data support a certain hypothesis and as such make an assessment of the significance. To quantify our degree of belief in a certain hypothesis H, we use the so called evidence

$$e(H|D,I) = 10\log_{10}\left[\frac{p(H|D,I)}{p(\overline{H}|D,I)}\right], \tag{3}$$

where $\overline{H}$ indicates hypothesis H to be not true. Due to the $\log_{10}$, this evidence reflects a decibel scale. In this context, the Bayesian observable $\psi \equiv -10\log_{10} p(D|H,I)$ and $\overline{\psi} \equiv -10\log_{10} p(D|\overline{H},I)$ are introduced. By combination of Eqs. (2) and (3) we obtain an expression for the evidence $e(\overline{H}|D,I)$ for any alternative to hypothesis H based on the data D and prior information I. In terms of the variables ψ and $\overline{\psi}$, this yields :

$$e(\overline{H}|D,I) = e(\overline{H}|I) + \psi - \overline{\psi} \leq e(\overline{H}|I) + \psi. \tag{4}$$

Eq. (4) implies that there is no alternative to a certain hypothesis H which can be supported by the data D by more than ψ decibel relative to H.

Let us now consider an experiment where the probabilities p_k corresponding to the various outcomes A_k on successive trials are independent and stationary. Such experiments belong to the so called Bernoulli class B_m [1]. The probability $p(n_1....n_m|B_m,I)$ of observing n_k occurrences of each outcome A_k after n trials is therefore given by the multinomial distribution :

$$p(D|B_m,I) = p(n_1....n_m|B_m,I) = \frac{n!}{n_1!....n_m!} p_1^{n_1}....p_m^{n_m}. \tag{5}$$

In terms of the Bayesian observable ψ we then obtain for each $H \in B_m$:

$$\psi_{B_m} = -10[\log_{10} n! + \sum_{k=1}^{m}(n_k \log_{10} p_k - \log_{10} n_k!)], \tag{6}$$

which is an exact expression!

In case the data is represented in histogram form, the above implies that n is the total number of entries, m represents the number of bins, n_k is the number of entries in bin k and p_k is the probability for an entry to fall in bin k. Once the various p_k are known, the ψ-value corresponding to a certain observed distribution can easily be obtained using Eq. (6).

In our investigation of AGN, a histogram will be populated according to the angular difference α of each neutrino arrival direction w.r.t. the source location in the sky. The data from a homogeneous background will follow a $\sin(\alpha)$ distribution, reflecting the solid angle effect.This obviously determines all p_k values once the angular bin size is chosen.

By performing off-source measurements and using Eq. (6), we obtain the distribution of the corresponding background ψ-values by randomizing these background data multiple times according to the solid angle distribution. By comparing the ψ-value of the on-source data with the background ψ-distribution we obtain the P-value or *significance* of our measurement. We can claim a source detection if the significance of a deviation from the background hypothesis has a P-value smaller than $5.73 \cdot 10^{-7}$, corresponding to a 5σ effect in case of a Gaussian distribution.

In case the observation does not lead to a significant detection, we determine an upper limit on the signal strength. To obtain such an upper limit we have worked out an exact analytical expression following a Bayesian approach using a uniform prior. The details of this procedure are provided hereafter.

4 Bayesian upper limit determination

To obtain an upper limit for a possible source flux, we first have to determine the upper limit for the source rate. Using Bayesian inference we obtain the full posterior PDF for the source rate and from that we can derive the corresponding flux PDF, via the concept of effective area, as explained hereafter.

In any experiment where events are recorded at a constant rate, the PDF for the number of observed events is described by a Poisson distribution. Our approach to obtain an upper limit is similar to the one outlined in [8], except that we have obtained an exact analytical expression without any approximation.

The data consist of on-source and off-source measurements, where the off-source data consist only of background events and the on-source data are a mix of background and source (*i.e.* signal) events.We start with the off-source analysis and use subsequently the obtained information as prior information in the on-source analysis. This implies that the current study is completely data driven and as such is a model independent search for a possible source signal.

4.1 Off-source measurements

Consider the case that in an off-source measurement N_{off} background events have been recorded over a time interval T_{off} with a constant background rate b. Using Eq.(2) we obtain the posterior background PDF by :

$$p(b|N_{\text{off}}, I) = \frac{p(b|I)p(N_{\text{off}}|b, I)}{p(N_{\text{off}}|I)}. \tag{7}$$

In the above equation the likelihood function $p(N_{\text{off}}|b, I)$ is given by the Poisson distribution corresponding to the measurement of N_{off} background events over a time span T_{off} at a constant rate b:

$$p(N_{\text{off}}|b, I) = \frac{(bT_{\text{off}})^{N_{\text{off}}} e^{-bT_{\text{off}}}}{N_{\text{off}}!}. \tag{8}$$

Since the integrated PDF amounts to 1 (*i.e.* $\int_{b_{\min}}^{b_{\max}} p(b|N_{\text{off}}, I)\,\mathrm{d}b = 1$), the normalisation factor $p(N_{\text{off}}|I)$ appearing in Eq. (7) is given by :

$$p(N_{\text{off}}|I) = \int_{b_{\min}}^{b_{\max}} p(b|I)p(N_{\text{off}}|b, I)\mathrm{d}b. \tag{9}$$

As mentioned before, $p(b|I)$ is the prior PDF for the background rate. For our analysis we use a uniform prior [8], which is given by

$$p(b|I) = \frac{1}{b_{\max} - b_{min}}. \tag{10}$$

The uniform prior attributes the same probability to each value of the background rate within the indicated range, reflecting our total ignorance about the actual background rate.

To cover the full range of possible background rates, the minimum value of the rate b is taken to be zero and Eq. (10) can be written as

$$p(b|I) = \frac{1}{b_{\max}}. \tag{11}$$

Using this expression for $p(b|I)$ together with Eqs. (8) and (9) we obtain an analytical expression for the normalisation factor

$$p(N_{\mathrm{off}}|I) = \int_0^{b_{\mathrm{max}}} \frac{1}{b_{\mathrm{max}}} \frac{(bT_{\mathrm{off}})^{N_{\mathrm{off}}} e^{-bT_{\mathrm{off}}}}{N_{\mathrm{off}}!} \mathrm{d}b. \tag{12}$$

Solving the above equation (for details see Appendix A1) we get :

$$p(N_{\mathrm{off}}|I) = \frac{1}{b_{\mathrm{max}}} \frac{\gamma(N_{\mathrm{off}}+1, b_{\mathrm{max}}T_{\mathrm{off}})}{N_{\mathrm{off}}!\, T_{\mathrm{off}}}, \tag{13}$$

where $\gamma(a,x)$ is the Incomplete Gamma function [9]. Substitution of Eqs. (8), (11) and (13) in Eq. (7) yields

$$p(b|N_{\mathrm{off}}, I) = \frac{T_{\mathrm{off}}(bT_{\mathrm{off}})^{N_{\mathrm{off}}} e^{-bT_{\mathrm{off}}}}{\gamma(N_{\mathrm{off}}+1, b_{\mathrm{max}}T_{\mathrm{off}})}, \tag{14}$$

which represents the posterior background rate PDF.

4.2 On-source measurements

Consider the case that in an on-source measurement N_{on} events, consisting of signal and background, have been recorded over a time interval T_{on} with a constant signal rate s and background rate b. Following Eq. (2) the joint probability of source and background is given by :

$$p(s,b|N_{\mathrm{on}}, I) = \frac{p(s,b|I)p(N_{\mathrm{on}}|s,b,I)}{p(N_{\mathrm{on}}|I)}. \tag{15}$$

Using the product rule [1] we can write the above equation as,

$$p(s,b|N_{\mathrm{on}}, I) = \frac{p(b|I)p(s|b,I)p(N_{\mathrm{on}}|s,b,I)}{p(N_{\mathrm{on}}|I)}, \tag{16}$$

where $p(b|I)$ is the prior probability for the background rate, which is in our case the posterior background PDF obtained from the off-source measurement reflected in Eq. (14). The likelihood function $p(N_{\mathrm{on}}|s,b,I)$ is the Poisson distribution for the combined signal and background rate $(s+b)$. The normalisation constant $p(N_{\mathrm{on}}|I)$ is obtained, as outlined in the previous section, by integrating the numerator of Eq. (16).

It is important to note that since the source rate s and the background rate b are independent, we can write $p(s|b,I) = p(s|I)$. Like for the background case discussed before, we use a uniform prior for $p(s|I)$, *i.e.*

$$p(s|I) = \frac{1}{s_{\mathrm{max}}} = p(s|b,I). \tag{17}$$

As before, this reflects our total ignorance about the source rate.

By substituting in Eq. (16) the expressions of Eq. (17) for $p(s|b,I)$, (14) for $p(b|I)$ and (8) for a total rate (s+b) we obtain the joint PDF for the source and background rates :

$$p(s,b|N_{\mathrm{on}}, I) = \frac{(bT_{\mathrm{off}})^{N_{\mathrm{off}}}\, e^{-bT_{\mathrm{off}}} \cdot (b+s)^{N_{\mathrm{on}}}\, e^{-(b+s)T_{\mathrm{on}}}}{\int_0^{b_{\mathrm{max}}} \int_0^{s_{\mathrm{max}}} (bT_{\mathrm{off}})^{N_{\mathrm{off}}}\, e^{-bT_{\mathrm{off}}} \cdot (b+s)^{N_{\mathrm{on}}}\, e^{-(b+s)T_{\mathrm{on}}}\, \mathrm{d}b\, \mathrm{d}s}. \tag{18}$$

However, we are interested in the posterior PDF for the source rate alone, independent of the background. The Bayesian formalism allows us to obtain this posterior PDF by marginalisation [1] of the joint PDF, Eq. (18), with respect to the background *i.e.*

$$p(s|N_{\mathrm{on}}, I) = \int_0^{b_{\mathrm{max}}} p(s,b|N_{\mathrm{on}}, I)\mathrm{d}b. \tag{19}$$

Solving the above integral we obtain an exact expression for the source rate posterior PDF (for details see Appendix A2) :

$$p(s|N_{\mathrm{on}}, I) = \frac{e^{-sT_{\mathrm{on}}} \sum_{i=0}^{N_{\mathrm{on}}} \frac{s^i (T_{\mathrm{on}}+T_{\mathrm{off}})^i \gamma(N-i+1, u_{\mathrm{max}})}{i!(N_{\mathrm{on}}-i)!}}{\sum_{j=0}^{N_{\mathrm{on}}} \frac{(T_{\mathrm{on}}+T_{\mathrm{off}})^j \gamma(N-j+1, u_{\mathrm{max}}) \gamma(j+1, s_{\mathrm{max}}T_{\mathrm{on}})}{j!(N_{\mathrm{on}}-j)!T_{\mathrm{on}}^{j+1}}}, \tag{20}$$

where $u_{\max} \equiv b_{\max}(T_{\text{on}} + T_{\text{off}})$ and $N \equiv N_{\text{on}} + N_{\text{off}}$.

In case no significant source signal is observed, Eq. (20) allows us to derive an upper limit for the source rate. As an example, the 90% source rate upper limit $s_{\text{u.l.}}$ is given by :

$$\int_0^{s_{\text{u.l.}}} p(s|N_{\text{on}}, I)\text{d}s = 0.9 \tag{21}$$

5 Analysis of ten nearby blazars

The approach presented in the current paper is tailored for sources with a constant signal rate. As such, our primary goal is the analysis of AGN which are expected to be steady sources of high-energy neutrinos and of which the locations are well known. By selecting a small region around each source location, several sky patches are defined from which data were collected to search for a possible deviation from the background "noise". The background is determined by performing observations of similar sky patches which do not coincide with AGN locations.

To validate the analysis procedure described in this report, we use the public data [10] of the muon neutrino candidate events recorded by the IceCube Neutrino Observatory [11,12] in its 40 string configuration (IC40), that collected data during the season 2008-2009. Our analysis was performed on ten nearby blazars (a special class of AGN with one of the jets pointing in the direction of the Earth) following the approach described in the previous sections. The blazars were selected from the online "Roma BZCAT Multi-frequency Catalogue of Blazars" [13] and are listed in Table 1. These blazars were chosen to be nearby, *i.e.* with a small redshift, and in the Northern hemisphere, to reduce the atmospheric muon background for the IceCube measurements.

We investigated each source individually and selected the recorded events within a 5° window around the source position. The 5° search area implies selecting all events within the 5σ angular uncertainty of the Icecube track reconstruction, which was determined to be of the order of 1° [12,14]. Note that the uncertainty on the blazar positions is less than an arcsecond.

Blazar Name	Right Ascension	Declination	Redshift	Distance [Mpc]
BZUJ1148+5924	177.20983	59.41567	0.011	46.2
BZUJ0048+3157	12.19642	31.95697	0.015	63
BZUJ0319+4130	49.95067	41.51169	0.018	75.6
BZUJ0319+4130	107.39246	50.18225	0.02	84
BZUJ0153+7115	28.35771	71.25181	0.022	92.4
BZUJ1719+4858	259.81025	48.98042	0.024	100.8
BZUJ1632+8232	248.13321	82.53789	0.025	105
BZUJ1715+5724	258.84579	57.41119	0.027	113.4
BZBJ1104+3812	268.95183	62.61225	0.027	113.4
BZUJ1755+6236	166.11379	38.20883	0.03	126

Table 1. Nearby blazars [13] used in the current analysis.

5.1 Bayesian assessment of significance

As outlined in [7], stacking the recorded events within the 5° cones of these ten blazars, according to their angular distance α from the actual blazar position, we obtain the distribution of events presented in Fig. 1. As mentioned in the previous sections, we need an expression for the various probabilities p_k of Eq. (6) to derive the ψ-value of the signal. In our case, the background is homogeneous and consequently the probabilities have to be consistent with the solid angle effect within our 5° cone, *i.e.* :

$$p_k = \frac{1}{1-\cos(5^\circ)}\left[\cos(w\cdot k) - \cos(w\cdot(k+1))\right], \tag{22}$$

where w is the width of each bin in our stacked histogram.

The stacked data, reflected in Fig. 1, comprised 407 events recorded over a time period of 375.5 days [15]. We have chosen 0.1° as angular bin width, which is well below the IceCube angular resolution of 1° so that our analysis can be regarded as unbinned. Using Eqs. (6) and (22) for a number of entries of $n = 407$ and a number of bins $m = 50$, the data represented in Fig. 1 yield $\psi_{observed} = 456.57\,\text{dB}$.

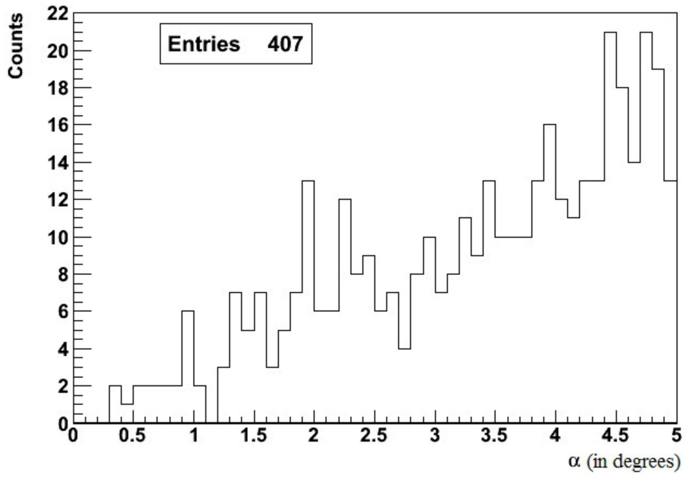

Fig. 1. The stacked distribution of events within a 5° cone of all our 10 Blazars of Table 1, with α the angle between the corresponding blazar location and the reconstructed arrival direction.

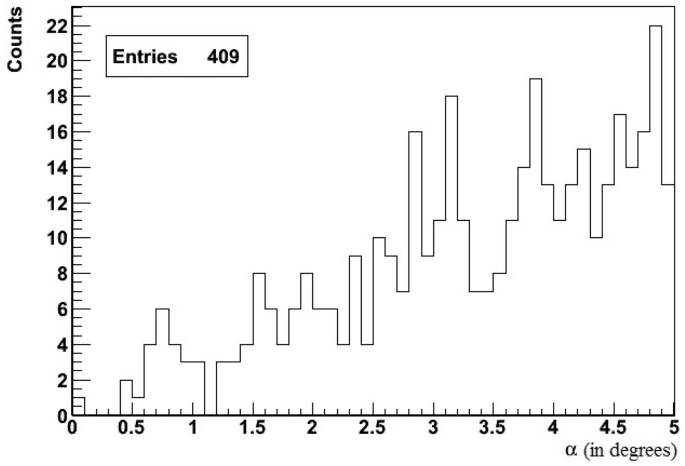

Fig. 2. The stacked distribution of events within a 5° off-source background region, 180° shifted in azimuth from the various blazar positions.

To quantify our belief that the stacked histogram represents only background, we need to compare this $\psi_{observed}$-value to the distribution obtained from the background only data. As the efficiency of IceCube is zenith angle dependent, we performed measurements of the background rate in 5° regions of the sky shifted from the various blazars positions only in the azimuth angle, keeping the zenith angle constant. However, the specific IC-40 configuration of IceCube is also azimuth angle dependent, so we made shifts of 180° in the azimuth angle to eliminate the azimuth angle dependence. The IC-40 sample has been taken over a detector live time period of 375.5 days, so that both the exposures for on-source, T_{on}, and off-source, $T_{\rm off}$, amount to 375.5 days. The off-source measurements yielded a total of 409 events. These stacked background measurements are shown in Fig. 2.

Randomising the background data 10^6 times according to the solid angle distribution, we obtain a distribution for the background ψ_{bkg}-values, which is presented in Fig. 3.

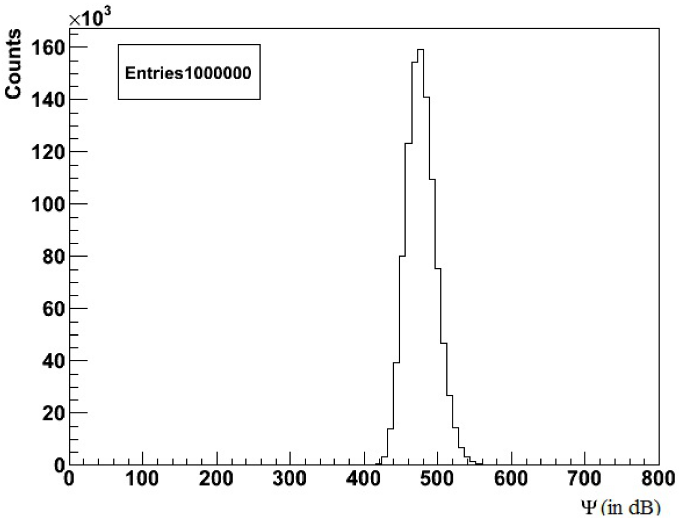

Fig. 3. The distribution of ψ-values of 10^6 randomizations of the background measurements.

Comparison of the actual observation $\psi_{observed}$ with the background distribution ψ_{bkg} yields the P-value of our measurement, which amounts to a P-value of 0.87. This implies that we cannot claim the presence of a signal. Consequently we will proceed to give an upper limit on the signal strength.

5.2 Upper limit determination using Uniform priors for Source and Background

5.2.1 Determination of the background rate

The posterior background rate PDF is obtained by substitution of the previously mentioned values of $T_{\rm off}$ and $N_{\rm off}$ in Eq. (14) and by using a sufficiently large value $b_{\rm max} = \frac{N_{\rm off}}{T_{\rm off}} \cdot 100 = 1.16$ mHz. The resulting background rate PDF is shown in Fig. 4.

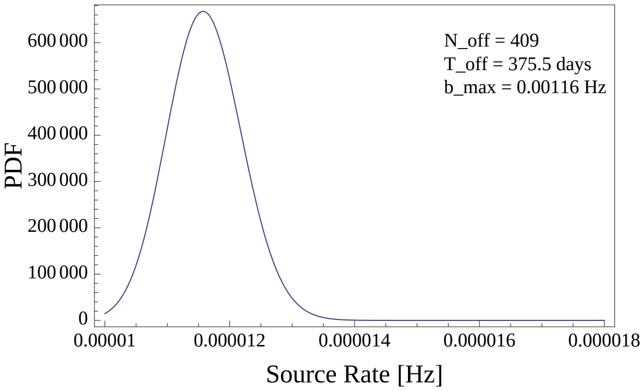

Fig. 4. Background rate PDF using a Uniform prior.

5.2.2 Determination of the source rate

The posterior source rate PDF is obtained by inserting the previously mentioned values of $T_{\rm on}$, $T_{\rm off}$, $N_{\rm on}$ and $N_{\rm off}$ in Eq. (20) and by using a sufficiently large value $s_{\rm max} = 1$ Hz. The resulting source rate PDF is shown in Fig. 5.

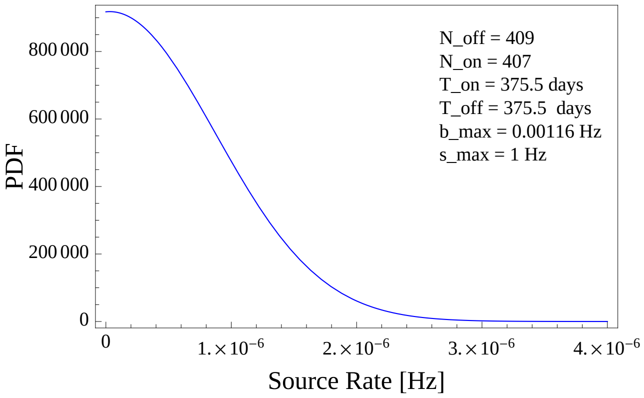

Fig. 5. Source rate PDF using a Uniform prior.

Using the PDF shown in Fig. 5 and applying Eq. (21), we obtain the 90% upper limit for the source rate :

$$s_{\mathrm{u.l.}} = 1.41 \times 10^{-6}\,\mathrm{Hz}. \tag{23}$$

Note that this rate does not take into account the reconstruction efficiency. The latter is taken into account by converting the source rate upper limit into a flux upper limit by means of the so called Effective Area, $\mathrm{A_{eff}}$, which is defined as

$$\mathrm{A_{eff}} = \frac{\text{number of observed events}}{\text{incoming flux}}. \tag{24}$$

By definition $\mathrm{A_{eff}}$ takes all reconstruction efficiencies into account. For the current analysis we use the angle averaged Effective Area, weighted by the observed energy estimate [10], which corresponds to $\mathrm{A_{eff}} = 9.95 \times 10^5\,\mathrm{cm}^2$. Our analysis was performed on a circular area of 5° centered on each of the 10 sources, representing in total $10 \times 0.0239\,\mathrm{sr} = 0.239\,\mathrm{sr}$. Together with the expressions (23) and (24) this leads to a 90% upper limit for the signal flux of $\Phi_{\mathrm{u.l.}} = \dfrac{s_{\mathrm{u.l.}}}{\mathrm{A_{eff}} \cdot 0.239} = 5.93 \times 10^{-12}\ \mathrm{s}^{-1}\,\mathrm{cm}^{-2}\,\mathrm{sr}^{-1}$.

However, this flux upper limit does not take into account the effect of neutrino oscillations. At the source we have $\nu_\mu : \nu_e : \nu_\tau = 2 : 1 : 0$ [15]. Assuming maximum oscillation we will observe on the Earth $\nu_\mu : \nu_e : \nu_\tau = 1 : 1 : 1$. A tiny fraction of the ν_τ will produce a muon which might also be detected in IceCube and as such have entered our event sample. However, we will neglect this effect since it is marginal and would require a special simulation which is beyond the scope of this paper. So our final value for the 90% upper limit for a signal flux is :

$$\Phi_{\mathrm{u.l.}} = 11.86 \times 10^{-12}\,\mathrm{s}^{-1}\,\mathrm{cm}^{-2}\,\mathrm{sr}^{-1}. \tag{25}$$

This upper limit may be directly compared to the result published by the IceCube Collaboration [15], which was obtained with a different analysis concerning a search for a diffuse high energy neutrino flux in the full Northern hemisphere: $\Phi_{\mathrm{u.l.}} = 8.89 \times 10^{-12}\ \mathrm{s}^{-1}\,\mathrm{cm}^{-2}\,\mathrm{sr}^{-1}$.

The limit obtained in this paper compares rather well to the above, and therefore indicates that the analysis method presented here is suitable to investigate neutrino fluxes from point sources.

6 Conclusion and Outlook

In this paper we have presented a mechanism to analyse point sources using data from neutrino telescopes following Bayesian inference. We have shown how to test a background only hypothesis using Bayesian statistics for sources like GRBs and AGN and we have provided a method to determine a possible constant source rate. For the latter we have worked out an exact analytical expression using uniform priors, that can readily be used to obtain the probability density function for the rate of any steady source. We have also shown how to obtain upper limits for the corresponding flux in case the observation does not lead to a significant signal.

Applying this method we analysed the public IceCube 40-string configuration data for 10 nearby blazars located in the Northern sky. We have found that the on-source data is consistent with a background only hypothesis. Therefore we have determined a 90% upper limit. Our upper limit agrees well with the previously published IceCube upper limit based on the same data set.

Furthermore, it is our intention to extend the current method also for non-steady sources like for instance GRBs. Apart from providing a signal significance for discovery [7], this should also provide a mechanism to accurately determine flux upper limits. The latter requires a non trivial extension of the method presented here, which is currently under study.

Acknowledgements

The authors would like to thank the IceCube Collaboration for providing the public data used in this report to evaluate our analysis method. This research was performed with financial support from the Odysseus programme of the Flemish Foundation for Scientific Research (FWO) under contract number G.0917.09.

Appendix A1

The normalisation factor of the posterior background rate PDF given in Eq. (12) may be written as :

$$p(N_{\mathrm{off}}|I) = \frac{1}{b_{\mathrm{max}}\, N_{\mathrm{off}}!} \int_0^{b_{max}} (bT_{\mathrm{off}})^{N_{\mathrm{off}}}\, e^{-bT_{\mathrm{off}}}\, \mathrm{d}b. \tag{26}$$

The integral part can be expressed as the so-called Incomplete Gamma function given by :

$$\gamma(a,x) = \int_0^x e^{-t}\, t^{a-1} \mathrm{d}t. \tag{27}$$

Using this expression, we can rewrite Eq. (26) as follows :

$$\begin{aligned} p(N_{\mathrm{off}}|I) &= \frac{1}{b_{\mathrm{max}}\, N_{\mathrm{off}}!} \int_0^{b_{\mathrm{max}}T_{\mathrm{off}}} (bT_{\mathrm{off}})^{N_{\mathrm{off}}}\, e^{-bT_{\mathrm{off}}}\, \frac{\mathrm{d}(bT_{\mathrm{off}})}{T_{\mathrm{off}}} & (28) \\ &= \frac{1}{b_{\mathrm{max}}} \frac{\gamma(N_{\mathrm{off}}+1, b_{\mathrm{max}}T_{\mathrm{off}})}{N_{\mathrm{off}}!\, T_{\mathrm{off}}}, & (29) \end{aligned}$$

which is the expression reflected in Eq. (13).

Appendix A2

According to Eq. (19) the posterior PDF for the source rate alone is given by :

$$p(s|N_{\mathrm{on}}, I) = \int_0^{b_{\mathrm{max}}} p(s,b|N_{\mathrm{on}}, I)\, \mathrm{d}b, \tag{30}$$

where

$$p(s,b|N_{\mathrm{on}}, I) = \frac{p(s|b,I)p(b|I)p(N_{\mathrm{on}}|s,b,I)}{p(N_{\mathrm{on}}|I)}.$$

Substitution of the various expressions given in section 4 yields :

$$p(s,b|N_{\mathrm{on}}, I) = \frac{\frac{1}{s_{\mathrm{max}}} \cdot \frac{T_{\mathrm{off}}(bT_{\mathrm{off}})^{N_{\mathrm{off}}} e^{-bT_{\mathrm{off}}}}{\gamma(N_{\mathrm{off}}+1, b_{\mathrm{max}}T_{\mathrm{off}})} \cdot \frac{(b+s)^{N_{\mathrm{on}}} T_{\mathrm{on}}^{N_{\mathrm{on}}} e^{-(b+s)T_{\mathrm{on}}}}{N_{\mathrm{on}}!}}{\int_0^{b_{\mathrm{max}}} \int_0^{s_{\mathrm{max}}} \frac{1}{s_{\mathrm{max}}} \cdot \frac{T_{\mathrm{off}}(bT_{\mathrm{off}})^{N_{\mathrm{off}}} e^{-bT_{\mathrm{off}}}}{\gamma(N_{\mathrm{off}}+1, b_{\mathrm{max}}T_{\mathrm{off}})} \cdot \frac{(b+s)^{N_{\mathrm{on}}} T_{\mathrm{on}}^{N_{\mathrm{on}}} e^{-(b+s)T_{\mathrm{on}}}}{N_{\mathrm{on}}!}\, \mathrm{d}b\, \mathrm{d}s}. \tag{31}$$

Combination of Eqs. (30) and (31) yields :

$$\begin{aligned} p(s|N_{\mathrm{on}}, I) &= \int_0^{b_{\mathrm{max}}} \frac{\frac{1}{s_{\mathrm{max}}} \cdot \frac{T_{\mathrm{off}}(bT_{\mathrm{off}})^{N_{\mathrm{off}}} e^{-bT_{\mathrm{off}}}}{\gamma(N_{\mathrm{off}}+1, b_{\mathrm{max}}T_{\mathrm{off}})} \cdot \frac{(b+s)^{N_{\mathrm{on}}} T_{\mathrm{on}}^{N_{\mathrm{on}}} e^{-(b+s)T_{\mathrm{on}}}}{N_{\mathrm{on}}!}}{\int_0^{b_{\mathrm{max}}} \int_0^{s_{\mathrm{max}}} \frac{1}{s_{\mathrm{max}}} \cdot \frac{T_{\mathrm{off}}(bT_{\mathrm{off}})^{N_{\mathrm{off}}} e^{-bT_{\mathrm{off}}}}{\gamma(N_{\mathrm{off}}+1, b_{\mathrm{max}}T_{\mathrm{off}})} \cdot \frac{(b+s)^{N_{\mathrm{on}}} T_{\mathrm{on}}^{N_{\mathrm{on}}} e^{-(b+s)T_{\mathrm{on}}}}{N_{\mathrm{on}}!}\, \mathrm{d}b\, \mathrm{d}s}\, \mathrm{d}b \\ &= \frac{\int_0^{b_{\mathrm{max}}} \frac{1}{s_{\mathrm{max}}} \cdot \frac{T_{\mathrm{off}}(bT_{\mathrm{off}})^{N_{\mathrm{off}}} e^{-bT_{\mathrm{off}}}}{\gamma(N_{\mathrm{off}}+1, b_{\mathrm{max}}T_{\mathrm{off}})} \cdot \frac{(b+s)^{N_{\mathrm{on}}} T_{\mathrm{on}}^{N_{\mathrm{on}}} e^{-(b+s)T_{\mathrm{on}}}}{N_{\mathrm{on}}!}\, \mathrm{d}b}{\int_0^{b_{\mathrm{max}}} \int_0^{s_{\mathrm{max}}} \frac{1}{s_{\mathrm{max}}} \cdot \frac{T_{\mathrm{off}}(bT_{\mathrm{off}})^{N_{\mathrm{off}}} e^{-bT_{\mathrm{off}}}}{\gamma(N_{\mathrm{off}}+1, b_{\mathrm{max}}T_{\mathrm{off}})} \cdot \frac{(b+s)^{N_{\mathrm{on}}} T_{\mathrm{on}}^{N_{\mathrm{on}}} e^{-(b+s)T_{\mathrm{on}}}}{N_{\mathrm{on}}!}\, \mathrm{d}b\, \mathrm{d}s} & (32) \\ &\equiv \frac{\mathrm{A}}{\mathrm{B}}. \end{aligned}$$

Considering the numerator of Eq. (32), we obtain :

$$\begin{aligned}
\mathrm{A} &= \int_0^{b\mathrm{max}} \frac{1}{s_{\max}} \cdot \frac{T_{\mathrm{off}}(bT_{\mathrm{off}})^{N_{\mathrm{off}}} e^{-bT_{\mathrm{off}}}}{\gamma(N_{\mathrm{off}}+1, b_{\max}T_{\mathrm{off}})} \cdot \frac{(b+s)^{N_{\mathrm{on}}} T_{\mathrm{on}}^{N_{\mathrm{on}}} e^{-(b+s)T_{\mathrm{on}}}}{N_{\mathrm{on}}!}\, \mathrm{d}b \\
&= \frac{1}{s_{\max}} \frac{T_{\mathrm{on}}^{N_{\mathrm{on}}} T_{\mathrm{off}}^{N_{\mathrm{off}}+1}}{N_{\mathrm{on}}!} \frac{1}{\gamma(N_{\mathrm{off}}+1, b_{\max}T_{\mathrm{off}})} \int_0^{b\mathrm{max}} (b+s)^{N_{\mathrm{on}}} b^{N_{\mathrm{off}}} e^{-(b+s)T_{\mathrm{on}}} e^{-bT_{\mathrm{off}}}\, \mathrm{d}b.
\end{aligned}$$

Using the Newtonian Binomial, $(a+b)^n = \sum_{i=0}^{n} \frac{n!}{i!(n-i)!} a^{n-i} b^i$, we find :

$$\mathrm{A} = \frac{1}{s_{\max}} \frac{T_{\mathrm{on}}^{N_{\mathrm{on}}} T_{\mathrm{off}}^{N_{\mathrm{off}}+1}}{N_{\mathrm{on}}!} \frac{1}{\gamma(N_{\mathrm{off}}+1, b_{\max}T_{\mathrm{off}})} \sum_{i=0}^{N_{\mathrm{on}}} \frac{N_{\mathrm{on}}!\, s^i\, e^{-sT_{\mathrm{on}}}}{i!(N_{\mathrm{on}}-i)!} \int_0^{b\mathrm{max}} b^{N_{\mathrm{on}}+N_{\mathrm{off}}-i} e^{-b(T_{\mathrm{on}}+T_{\mathrm{off}})}\, \mathrm{d}b.$$

Using the Incomplete Gamma function, Eq. (27), and simplifying the above equation, we finally find

$$\mathrm{A} = \frac{1}{s_{\max}} \frac{T_{\mathrm{on}}^{N_{\mathrm{on}}} T_{\mathrm{off}}^{N_{\mathrm{off}}+1}}{\gamma(N_{\mathrm{off}}+1, b_{\max}T_{\mathrm{off}})} \sum_{i=0}^{N_{\mathrm{on}}} \frac{s^i\, e^{-sT_{\mathrm{on}}}}{i!(N_{\mathrm{on}}-i)!} \frac{\gamma(N-i+1, u_{\max})}{(T_{\mathrm{on}}+T_{\mathrm{off}})^{N_{\mathrm{on}}+N_{\mathrm{off}}-i+1}}, \tag{33}$$

where $u_{\max} = b_{\max}(T_{\mathrm{on}}+T_{\mathrm{off}})$ and $N = N_{\mathrm{on}} + N_{\mathrm{off}}$.

Applying the same procedure, we obtain for the denominator :

$$\begin{aligned}
\mathrm{B} &= \int_0^{b\mathrm{max}} \int_0^{s\mathrm{max}} \frac{1}{s_{\max}} \cdot \frac{T_{\mathrm{off}}(bT_{\mathrm{off}})^{N_{\mathrm{off}}} e^{-bT_{\mathrm{off}}}}{\gamma(N_{\mathrm{off}}+1, b_{\max}T_{\mathrm{off}})} \cdot \frac{(b+s)^{N_{\mathrm{on}}} T_{\mathrm{on}}^{N_{\mathrm{on}}} e^{-(b+s)T_{\mathrm{on}}}}{N_{\mathrm{on}}!}\, \mathrm{d}b\, \mathrm{d}s \\
&= \int_0^{s\mathrm{max}} N\, \mathrm{d}s \\
&= \frac{1}{s_{\max}} \frac{T_{\mathrm{on}}^{N_{\mathrm{on}}} T_{\mathrm{off}}^{N_{\mathrm{off}}+1}}{\gamma(N_{\mathrm{off}}+1, b_{\max}T_{\mathrm{off}})} \sum_{j=0}^{N_{\mathrm{on}}} \frac{1}{j!(N_{\mathrm{on}}-j)!} \frac{\gamma(N-j+1, u_{\max})}{(T_{\mathrm{on}}+T_{\mathrm{off}})^{N_{\mathrm{on}}+N_{\mathrm{off}}-j+1}} \int_0^{s\mathrm{max}} s^j\, e^{-sT_{\mathrm{on}}}\, \mathrm{d}s \\
&= \frac{1}{s_{\max}} \frac{T_{\mathrm{on}}^{N_{\mathrm{on}}} T_{\mathrm{off}}^{N_{\mathrm{off}}+1}}{\gamma(N_{\mathrm{off}}+1, b_{\max}T_{\mathrm{off}})} \sum_{j=0}^{N_{\mathrm{on}}} \frac{1}{j!(N_{\mathrm{on}}-j)!} \frac{\gamma(N-j+1, u_{\max})}{(T_{\mathrm{on}}+T_{\mathrm{off}})^{N_{\mathrm{on}}+N_{\mathrm{off}}-j+1}} \frac{\gamma(j+1, s_{\max}T_{\mathrm{on}})}{T_{\mathrm{on}}^{j+1}}.
\end{aligned}$$

Which finally gives, after simplification, for the posterior source rate probability density function :

$$p(s|N_{\mathrm{on}}, I) = \frac{e^{-sT_{\mathrm{on}}} \sum_{i=0}^{N_{\mathrm{on}}} \frac{s^i\, (T_{\mathrm{on}}+T_{\mathrm{off}})^i\, \gamma(N-i+1, u_{\max})}{i!(N_{\mathrm{on}}-i)!}}{\sum_{j=0}^{N_{\mathrm{on}}} \frac{(T_{\mathrm{on}}+T_{\mathrm{off}})^j\, \gamma(j+1, s_{\max}T_{\mathrm{on}})\, \gamma(N-j+1, u_{\max})}{j!(N_{\mathrm{on}}-j)!\, T_{\mathrm{on}}^{j+1}}}. \tag{34}$$

References

[1] E.T. Jaynes, Probability Theory, Cambridge University Press, Cambridge, 2003.

[2] E. D. Feigelson and G. J. Babu, Statistical Challenges in Modern Astronomy III, Springer, Heidelberg, 2002.

[3] C. Arina, Bayes and present dark matter direct search status, J. Phys. Conf. Ser. **375** (2012) 012009 [arXiv:1110.0313].

[4] G. D'Agostini, Bayesian reasoning in high-energy physics: Principles and applications, CERN-YELLOW-99-03, Geneva, 1999.

[5] R. D. Cousins, Why isn't every physicist a Bayesian?, Am. J. Phys. **63** (1995) 398.

[6] T. Bayes and Mr. Price, An Essay towards solving a Problem in the Doctrine of Chances, Phil. Trans. **53** (1763) 370418.

[7] N. van Eijndhoven, On the Observability of High-Energy Neutrinos from Gamma Ray Bursts, Astropart. Phys. **28** (2008) 540-546 [arXiv:astro-ph/0702029v2].

[8] P. Gregory, Bayesian Logical Data Analysis for the Physical Sciences, Cambridge University Press, Cambridge, 2010.

[9] G. B. Arfken and H. J. Weber, Mathematical Methods for Physicists, Harcourt/Academic Press, San Diego, 2001.

[10] http://icecube.wisc.edu/science/data/ic40.

[11] F. Halzen and S. R. Klein, IceCube: An Instrument for Neutrino Astronomy, Rev. Sci. Instrum. **81** (2010) 081101 [arXiv:1007.1247v2].

[12] J. Ahrens *et al.*, IceCube Collaboration, Sensitivity of the IceCube detector to astrophysical sources of high energy muon neutrinos, Astropart. Phys. **20** (2004) 507-532 [arXiv:astro-ph/0305196].

[13] http://www.asdc.asi.it/bzcat/.

[14] R. Abbasi *et al.*, IceCube Collaboration, The Shadow of the Moon in Cosmic Rays measured with IceCube, Proc. of the 32nd International Cosmic Ray Conference V4 (2011) 264-267 [arXiv:1111.2741].

[15] R. Abbasi *et al.*, IceCube Collaboration, A Search for a Diffuse Flux of Astrophysical Muon Neutrinos with the IceCube 40-String Detector, Phys. Rev. D **84** (2011) 082001 [arXiv:1104.5187].